GCM SIMULATIONS OF THE MARS NORTH POLAR CAP SPRINGTIME RETREAT

F. Daerden, L. Neary, *Belgian Institute for Space Aeronomy, Brussels, Belgium (contact: frank.daerden@aeronomie.be)*, **B. Cantor,** *Malin Space Science Systems, San Diego, USA,* **T. Appéré**, *IPAG, UMR 5274, Grenoble, France.*

Introduction:

The annual retreat of the seasonal north polar cap during local springtime is a phenomenon which has been observed since the times of only Earth-based visual telescopic observations, e.g. Antoniadi (1930), Dollfus (1973), Iwasaki et al. (1979). Instruments in orbit in the space age have monitored the event with high precision. We analyze the retreat as simulated in a 3D Global Circulation Model for Mars, GEM-Mars, and compare it to a selection of datasets (MARCI, OMEGA, TES, THEMIS, GRS). The so-called water ice annulus, a zone of water ice deposited on the surface around the CO_2 ice cap, is also simulated. Comparisons with purely visible datasets only allow for a comparison of the extended polar cap zone (CO_2+H_2O ice zones). IR sensitive sensors (TES, THEMIS, OMEGA) provide additional information on the boundaries of the CO_2 and H_2O ice cap regions.

The temporal evolution of the seasonal cap retreat during local springtime is simulated in reasonable agreement with the datasets, but additional work is needed on the precise simulation of the surface water ice.

The GEM-Mars 3D GCM:

The Global Environmental Multiscale model for Mars (GEM-Mars) is a 3D gridpoint global circulation model (GCM) for Mars based on the terrestrial community model GEM, which is used for operational weather forecasting by the Meteorological Service of Canada (Coté et al. 1998). A first version of GEM adapted for Mars was the GM3 model of Moudden and McConnell (2005). New physics routines were added by Akingunola (PhD, 2008) and since 2009 at the Belgian Institute for Space Aeronomy. GEM-Mars is typically run on a 4°x4° uniform grid and has 102 hybrid levels ranging from the surface to ~150 km. GEM-Mars has an interactive 14 layer soil model including a subsurface ice table, a surface layer treatment following Monin-Obhukov similarity theory, a roughness length map (Hébrard et al. 2012) implemented on the sub-grid scale, a parameterization for the convective boundary layer (Holtslag and Boville, 1993), active dust-, CO_2-, pressure- and water cycles, a low level blocking scheme and gravity wave drag parameterization (Zadra et al. 2003), and online photochemistry (Garcia-Munoz et al. 2005, Neary et al., this workshop). Also routines for active dust lifting by saltation and dust devils were recently implemented in GEM-Mars (Daerden et al., this workshop).

In order to manage the high resolution geophysical fields (albedo, thermal inertia, roughness length) in the framework of the coarser GCM, subgrid scale treatments were developed based on a histogram method. This is a first step towards a subgrid scale treatment of the permanent north polar water ice cap.

Polar cap formation:

The CO_2 ice formation is implemented in GEM-Mars in a way similar to the original work of Forget et al (1998). The heat flows between atmosphere and surface are proportional to the thermal inertia (data from TES). The factor of proportionality is physically related to the surface heat capacity, and by imposing the soil volumetric heat capacity, it is related to the depth of the heat exchange region. The CO_2 ice is formed by instantaneous condensation in the atmosphere and the sedimentation occurs through an instant cascade. Also direct freezing onto the surface is taken into account.

The polar cap simulation needs to be done such that it simultaneously complies with several observational constraints, e.g.:

- the radius of the visible cap and the related latitude coverage, provided by MARCI images (Cantor et al. 2010);
- the total CO_2 ice mass in the polar caps, provided by MOD/GRS (Kelly et al. 2006);
- the pressure variation (which is calculated interactively in the GCM), provided by Viking Lander and Phoenix lander (Taylor et al. 2010) surface pressure measurements.

Furthermore data from Wagstaff et al. (2008), using THEMIS and TES, and Appéré et al. (2011) using OMEGA, provide more in-depth analysis of the composition of the cap, in terms of bulk CO_2 ice and the surrounding water ice annulus. This imposes important new constraints in addition to the ones listed above.

The water cycle in the present GCM starts with a permanent water ice cap in the north which releases water vapor as a tracer emitted in the surface layer and subsequently following the resolved general circulation. Formation of ice occurs in the atmosphere (freezing into 2 µm particles with explicit treatment of sedimentation) as well as by direct freezing onto the surface (see also Neary et al., this workshop).

Polar cap simulations:

The simulations start at L_s=0° from a model state coming from previous multi-annual model runs. The CO_2 cycle reaches a state which is consistent with the CO_2 ice mass cycle from GRS (Kelly et al. 2006, Haberle et al. 2008). Also the surface pressure cycle becomes consistent with the measurements of the Viking Landers, the Phoenix lander (Taylor et al. 2010) and MGS/TES (Smith, 2004).

While the GCM produces an atmospheric water cycle in reasonable agreement with the measurements of TES (see Neary et al., this workshop), it currently underestimates surface water ice in the northern subpolar regions. This may be related to an implementation problem, a non-optimization of model parameters (e.g. the imposed albedo of the surface water ice, currently set to 0.36), or it may simply need more spin-up time (e.g. Richardson and Wilson, 2002). This is work in progress.

Figure 1 compares the equivalent radius of the seasonal north polar cap to data derived from MARCI images (Cantor et al. 2010). MARCI will only detect the total visible cap, which is composed of a bulk region of CO_2 ice and a surrounding water ice annulus. When the surface water ice is increased in the initial conditions, the correspondence to the MARCI cap radius is better (green curves).

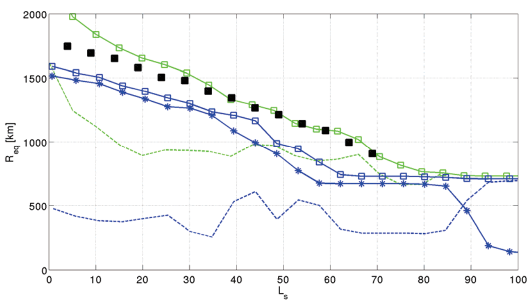

Figure 1: Simulation of the seasonal north polar cap radius compared to MARCI results for MY29 (black squares). Star symbols represent the CO_2 ice area, and dashed lines the surface water ice outside of the CO_2 area. Square symbols represent the total visible cap in the simulations. Blue: simulation with low initial surface water ice; green: simulation with increased initial surface water ice.

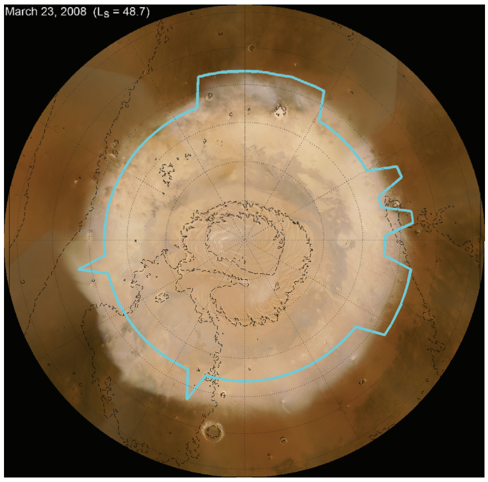

Figure 2: MARCI mosaic image for L_s=48.7° showing the seasonal north polar cap. The added contour represents the outer edge of the water ice annulus as simulated in GEM-Mars.

A direct comparison between the visible cap simulation and MARCI is shown in Figure 2.

IR sensors such as THEMIS and OMEGA can provide more information on the composition of the cap (Wagstaff et al. 2008, Appéré et al. 2011). Here we focus on the comparison of the GEM-Mars simulations with OMEGA.

Figure 3 shows some initial results. The CO_2 ice boundary in the GCM is located too far to the north, although the average deviation from the data is comparable to the horizontal grid resolution of the model (4 degrees). The water ice annulus is comparable in range to the values reported in Wagstaff et al. (2008), but only for the simulation with enhanced initial surface water ice.

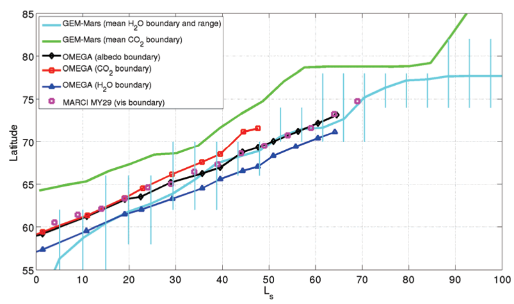

Figure 3: Comparison of the GEM-Mars simulation results to OMEGA and MARCI (MY29) data, for the zonally averaged limits of the different regions in the seasonal cap. As explained in

Appéré et al. (2011) the model CO_2 boundary has to be compared to the OMEGA albedo boundary. The vertical lines represent the latitude range of the water ice annulus in the GCM (simulation with enhanced initial surface water ice).

Conclusions:

The GEM-Mars model produces a CO_2 cycle in reasonable agreement with the polar ice mass measurements from GRS (Kelly et al. 2006). The present work is trying to improve our understanding of the spatial extent of the simulated cap, with specific focus on the springtime retreat of the seasonal north polar cap. Early simulations presented here indicate that the latitudinal coverage of the cap is too small in comparison to the results from OMEGA (Appéré et al. 2011), but the typical deviation is comparable to the resolution of the model grid. More problematic is the simulation of the surface water ice. In the current standard model simulation the water ice annulus is too small. Only by imposing enhanced initial conditions for the surface water ice, the simulation of the polar cap, including the water ice annulus, becomes comparable to the measurements from MARCI and OMEGA. Future work includes improving the simulation of the surface water ice.

References:

Akingunola, A. (2008), Martian Water Cycle Modeling with the Second Generation of the Global Mars Multiscale Model, PhD thesis, York University

Antoniadi, E.M. (1930), La Planète Mars. Herman, Paris, France, pp. 47–314.

Appéré, T., et al. (2011), Winter and spring evolution of northern seasonal deposits on Mars from OMEGA on Mars Express, J. Geophys. Res., 116, E05001

Cantor, B.A., et al (2010), MARCI and MOC observations of the atmosphere and surface cap in the north polar region of Mars, Icarus 208, 61–81

Côté, J., et al (1998), The operational CMC-MRB Global Environmental Multiscale (GEM) model: Part I—Design considerations and formulation, Mon. Weather Rev., 126, 1373–1395

Dollfus, A. (1973), New optical measurements of planetary diameters IV. Size of the North Polar Cap of Mars. Icarus 18, 142–155.

Forget, F., et al. (1998), CO_2 Snowfall on Mars: Simulation with a General Circulation Model, Icarus 131, 302–316

García-Muñoz, A., et al. (2005), Airglow on Mars: Some model expectations for the OH Meinel bands and the O2 IR atmospheric band, Icarus 176, 75–95

Haberle, R.M., et al. (2008), The effect of ground ice on the Martian seasonal CO_2 cycle, Planet. Sp. Sci. 56, 251–255

Hébrard, E., et al. (2012), An aerodynamic roughness length map derived from extended Martian rock abundance data, J. Geophys. Res., 117, E04008

Holtslag, A. A. M. and B. A. Boville (1993), Local versus nonlocal boundary-layer diffusion in a global climate model. J. Climate, 6, 1825–1842.

Iwasaki, K., et al. (1979), Behavior of the Martian North Polar Cap 1975–1978. J. Geophys. Res. 84, 8311–8316.

Kelly, N.J., et al. (2006), Seasonal polar carbon dioxide frost on Mars: CO_2 mass and columnar thickness distribution, J. Geophys. Res., 111, E03S07

Moudden, Y. and J.C. McConnell (2005), A new model for multiscale modeling of the Martian atmosphere, GM3, J. Geophys. Res. 110, E04001.

Richardson, M.I., and R.J. Wilson (2002), Investigation of the nature and stability of the Martian seasonal water cycle with a general circulation model, J. Geophys. Res. 107, E5, 5031.

Smith, M.D. (2004), Interannual variability in TES atmospheric observations of Mars during 1999–2003, Icarus 167, 148–165

Taylor, P. A., et al. (2010), On pressure measurement and seasonal pressure variations during the Phoenix mission, J. Geophys. Res., 115, E00E15

Wagstaff, K.L., et al. (2008), Observations of the north polar water ice annulus on Mars using THEMIS and TES, Planet. Sp. Sci. 56, 256–265

Zadra, A., et al. (2003): The subgrid-scale orographic blocking parametrization of the GEM Model, Atmosphere-Ocean, 41:2, 155-170.